Note deals with the application of base burning in v channels attached to the base of a noncircular missile for base-drag reduction.

Experimental Facility And Model

All experiments were conducted at Mach 2 in a Wichita State University 23×23-cm supersonic blowdown wind tunnel. Air for all tests was supplied from storage tanks of 20-m^3 capacity and a maximum storage pressure of 1724 kN/m^2. To reduce the humidity of air in the test section, a water cooled heat exchanger and a centrifugal water separator were installed just downstream of the compressor. Gaseous hydrogen for base burning was supplied from a commercial high-pressure cylinder at room temperature. Hydrogen mass-flow rate was monitored by a set of calibrated in-line flow nozzles. Pressure drop across the nozzle was measured by a differential-type pressure transducer.

Since the termination of a flat surface into a v channel was a prerequisite for the stable vortices to form in the v channel, a hexagonal cross-section missile was designed primarily to facilitate the utilization of six v channels in the base of the missile. This geometry guaranteed the formation of the vortex system in the bottom of the v channel where hydrogen was injected and burned. To reduce the interference due to reflected shock waves, the overall length of the model with the v channels attached was 300 mm, which was less than the distance at which the shock waves reflected from the tunnel walls were anticipated to hit. This was later confirmed by schlieren images. The model width (across flat sides) was 51 mm and was designed to slide on an upstream support to which strain-gauged flexures were attached for drag measurement (Fig 2). The balance was calibrated before and after each series of tests for possible dc shift and hysteresis. Six v channels with v angle of 60 deg were soldered to a steel base plate that was attached to the model base. Each v channel was 76 mm long and 24 mm deep. In the middle of the base plate, a spark igniter was inserted through a 4-mm hole. Hydrogen was uniformly supplied to each channel separately from a built-in manifold.

Under the given capacity of storage tanks, a typical run time was approximately 14 s for a Mach 2 flow. Tunnel stagnation pressure and temperature were held constant at 483 kN/m2 and 293 K, respectively, resulting in a test Reynolds number of 20×10^6 based on model length. After the flow was established in the test section, the hydrogen supply valve and an analog X/Y plotter were activated to record the output from the strain-gauge balance. The spark igniter was used only momentarily to the ignite hydrogen. Force data were obtained from the time histories, specific impulse and hydrogen mass-flow rate were calculated after each run.

Results And Discussion

The time histories of the test runs indicated that the injection alone was contributing very little to the changes in drag readings and that a large part of the reduction was due to burning. This is possibly due to the presence of v channels in the base that act as splitter plates and therefore increase the base pressure. Because of the physical constraints of the model size and the difference in the type of flows (axisymmetric vs three dimensional), no attempts were made to measure model drag without v channels.

During the initial tests, difficulty was encountered in achieving stable burning due to the small reaction time of hydrogen. To increase the residence time of hydrogen in the base region, flow deflectors were installed on each supply port to direct hydrogen toward the bottom of the v channels. Stable burning was thus achieved for all hydrogen supply pressures. These deflectors also served the purpose of eliminating the axial momentum of the hydrogen jet, which would have otherwise opened the wake or altered the vortical flow within v channels.

Analysis of time records and flow parameters indicated that the error in the hydrogen mass-flow measurement remained below 4% and the drag readings were observed to be repeating well within 3%. The overall error was estimated to be $< 5\%$.

The percentage drag reduction and specific impulse is plotted against the nondimensionalized hydrogen mass-flow rate in Fig. 3. An average drag reduction of 30% was achieved with this method of base burning proving the effectiveness of v channels as an alternate method of wake modification. In addition, a very high specific impulse was also achieved which is compatible with the analytical results of Zumwalt et al.[5]

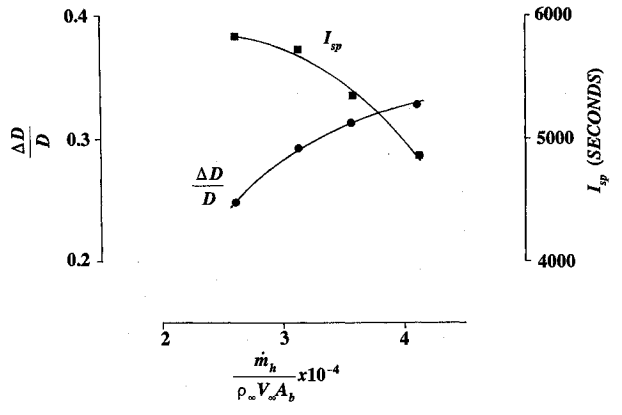

Fig. 3 Effective drag reduction and specific impulse obtained at different nondimensionalized hydrogen mass-flow rates.

References

[1]Barr, G. L., Experimental Investigation of the Sudden Expansion of a Supersonic Plane Flow into a 90 Degree Vee Channel," M.S. Thesis, Wichita State University, Wichita, KS, May 1972.

[2]Zumwalt, G. W., "Experiments in Three-Dimensional Separating and Reattaching Flows," AIAA Paper 81-0259, Jan. 1981

[3]Zumwalt, G. W., "Supersonic Burning in Separated Flow Regions," Aeronautical Rpt. 82-2, Wichita State University, Wichita, KS, Aeronautical Rpt. 82-2, April 1982.

[4]Friedberg, R. and Ahmed A., "3-D Supersonic Combustion Experiments with Hydrogen in V-Trough," AIAA Paper 82-0417, Jan. 1982.

[5]Zumwalt, G. W., Tang, H. H., and Denny, S. C., "Analysis of Base Burning Methods and Applications," Workshop on Aerodynamics of Base Combustion, Purdue Univ., West Lafayette, IN, May 1974.

Solar Sail Trajectories at the Lunar L_2 Lagrange Point

Colin R. McInnes*
University of Glasgow, Glasgow G12 8QQ, Scotland, United Kingdom

Introduction

THE concept of solar sailing came to fruition in the mid-1970s when it was adopted by NASA as a possibility for a comet Halley rendezvous mission.[1] During this time much work was carried out on the optimization of two-body solar sail dynamics for interplanetary trajectories.[2] More recently, interest has arisen in "exotic" solar sail trajectories with novel mission applications. Work by Forward[3] has shown that high-performance solar sails may have useful applications for terrestrial communications purposes. Currently, McInnes and Simmons are investigating large new families of solar sail

Received Nov. 19, 1991; revision received April 10, 1991; accepted for publication June 9, 1991.

*Space Systems Group, Department of Aerospace Engineering.

trajectories such as Sun-centered halo-type orbits,[4,5] with the sail executing a circular orbit of a chosen period above the ecliptic, and analogous Earth-centered halo orbits.[6]

Although these trajectories require advanced sail designs and materials, it is timely to investigate what exotic trajectories may be flown with current sail concepts, such as the solar sails being designed for the proposed Moon race.[7] It is therefore the purpose of this Note to demonstrate the possibility of such an exotic trajectory. It will be shown that, with a suitable sail attitude control program, a 3.5×10^3 km displaced, out-of-plane halo-type trajectory around the Earth-Moon L_2 point may be executed with sail accelerations of only 0.2 mms^{-2}. Such a trajectory could be used in future lunar far-side communications in advanced lunar operations in a similar manner to the "hummingbird" concept of Vonbun.[8] At the Earth-Sun L_1 point, the same sail could be displaced into a modified equilibrium point 1.2×10^6 km above the ecliptic plane, demonstrating the use of sails for solar radio disk avoidance in Lagrange point space science missions.

Three-body Solar Sail Dynamics

We will consider now an idealized, perfectly reflective solar sail in a corotating reference frame of constant angular velocity Ω with the Earth and Moon m_1, m_2 in circular orbit as shown in Fig. 1. The sail attitude is defined by a unit vector n normal to the sail surface and fixed in the corotating frame. The magnitude of the solar radiation pressure force exerted on the sail is given by the sail characteristic acceleration a_0. It will be assumed that a_0 is constant over the scale of the problem. This acceleration depends directly on the total mass (sail + payload) per unit area of the spacecraft σ. By considering the momentum flux, it may be shown that $a_0 = 2P/\sigma$, where $P = 4.5 \times 10^{-6}$ Nm^{-2} is the solar radiation pressure at 1 AU. The units of the problem are chosen in the usual way such that the gravitational constant, the Earth-Moon distance, the sum of the Earth and lunar masses, and so the angular velocity of corotation are all unity.

The vector equation of motion for the solar sail in this corotating frame may be written as

$$\frac{d^2\boldsymbol{r}}{dt^2} + 2\boldsymbol{\Omega} \times \frac{d\boldsymbol{r}}{dt} + \nabla U(\boldsymbol{r}) = \boldsymbol{a} \tag{1}$$

where the corotating three-body potential $U(\boldsymbol{r})$ and the radiation pressure acceleration $\boldsymbol{a}$ are given by

$$U(\boldsymbol{r}) = -(\tfrac{1}{2}|\boldsymbol{\Omega} \times \boldsymbol{r}|^2 + \frac{1-\mu}{r_1} + \frac{\mu}{|r_2|}), \quad \boldsymbol{a} = a_0(\boldsymbol{S}.\boldsymbol{n})^2\boldsymbol{n} \tag{2}$$

with $\mu = (m_2/m_1 + m_2) = 0.01215$, the mass ratio of the Earth-Moon system. The sail attitude is constrained such that $\boldsymbol{S}.\boldsymbol{n} \geq 0$ and the direction of the Sun line is given by

$$\boldsymbol{S} = [\cos(\Omega_* t), \ -\sin(\Omega_* t), \ 0] \tag{3}$$

where $\Omega_* = 0.9252$ is the angular rate of the Sun line in the corotating frame in dimensionless units. The small annual changes (± 5 deg) in the inclination of the Sun line with respect to the plane of the system are ignored.

We will now investigate the dynamics of the sail in the neighborhood of the L_2 point at r_L. Perturbing the system of Eqs. (1) such that $\boldsymbol{r} \to \boldsymbol{r}_L + \boldsymbol{\delta}$, we obtain

$$\frac{d^2\boldsymbol{\delta}}{dt^2} + 2\boldsymbol{\Omega} \times \frac{d\boldsymbol{\delta}}{dt} + \nabla U(\boldsymbol{r}_L + \boldsymbol{\delta}) = \boldsymbol{a}(\boldsymbol{r}_L + \boldsymbol{\delta}) \tag{4}$$

where $\boldsymbol{\delta} = (\xi,\eta,\zeta)$ represent small displacements from the L_2 point in the (x,y,z) directions. The potential gradient may be Taylor expanded about the L_2 point to first order as

$$\nabla U(\boldsymbol{r}_L + \boldsymbol{\delta}) = \nabla U(\boldsymbol{r}_L) + \frac{\partial}{\partial \boldsymbol{r}} \nabla U(\boldsymbol{r})\,|\boldsymbol{\delta} + 0(|\boldsymbol{\delta}|^2) \qquad \boldsymbol{r} = \boldsymbol{r}_L \tag{5}$$

Then, since $\nabla U(\boldsymbol{r}_L) = \boldsymbol{0}$ and $\partial \boldsymbol{a}/\partial \boldsymbol{r} = 0$ (since the radiation field is assumed uniform), we obtain a linear variational system, viz.,

$$\frac{d^2\boldsymbol{\delta}}{dt^2} + \mathbf{M}_1 \frac{d\boldsymbol{\delta}}{dt} + \mathbf{M}_2\,\boldsymbol{\delta} = \boldsymbol{a} \tag{6}$$

where $\boldsymbol{M}_2$ is the gravity gradient tensor in Eq. (5) and the skew symmetric gyroscopic matrix $\boldsymbol{M}_1$ is given by

$$\boldsymbol{M}_1 = \begin{bmatrix} 0 & -2 & 0 \\ 2 & 0 & 0 \\ 0 & 0 & 0 \end{bmatrix} \quad \boldsymbol{M}_2 = (U^0{}_{ij}), \ i,j = x,y,z \tag{7}$$

where $U^0{}_{ij}$ is the (i,j) partial derivative of the potential with respect to the Cartesian axes, evaluated at the L_2 point.

The sail attitude is now fixed such that the sail normal points along the Sun line but is pitched at an angle γ to the plane of the system, Fig. 2. With this choice of attitude control program, Eq. (6) may then be written in component form as

$$\frac{d^2\xi}{dt^2} - 2\frac{d\eta}{dt} + U^0{}_{xx}\xi = a_0 \cos(\Omega_* t)\cos^3\gamma \tag{8a}$$

$$\frac{d^2\eta}{dt^2} + 2\frac{d\xi}{dt} + U^0{}_{yy}\eta = -a_0 \sin(\Omega_* t)\cos^3\gamma \tag{8b}$$

$$\frac{d^2\zeta}{dt^2} + U^0{}_{zz}\zeta = a_0 \cos^2\gamma \sin\gamma \tag{8c}$$

The complete solution of Eqs. (8) will in general have divergent modes giving unbound motion. Therefore, since the instability time scale at the L_2 point is 12.7 days, active control via feedback to the sail is required to suppress these modes. We require then a particular periodic in plane solution of the form

$$\xi(t) = \xi_0 \cos(\Omega_* t), \quad \eta(t) = \eta_0 \sin(\Omega_* t) \tag{9}$$

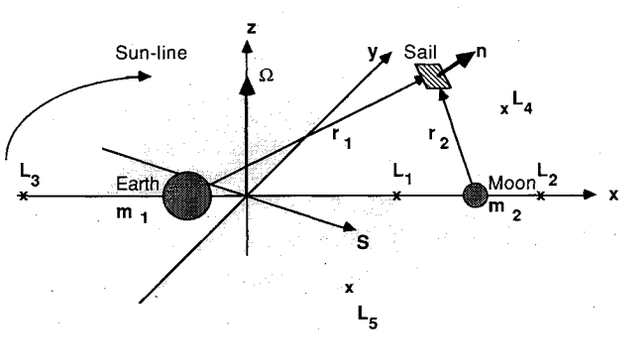

Fig. 1 Schematic geometry of the Earth-Moon restricted three-body problem.

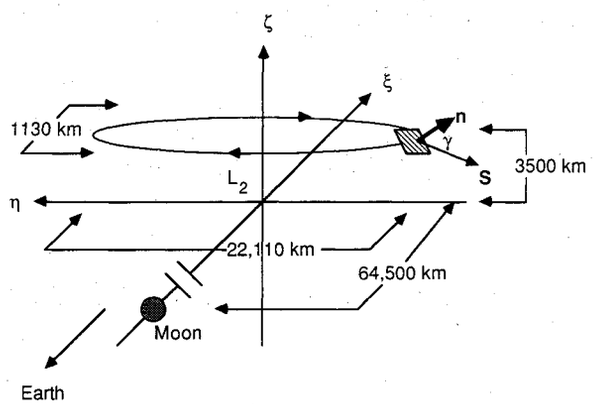

Fig. 2 Out-of-plane solar sail trajectory at the lunar L_2 point.

as used by Farquhar.[9] The required periodic solution is substituted in Eqs. (8) to give

$$\begin{Bmatrix} \xi_0 \\ \eta_0 \end{Bmatrix} = -\begin{Bmatrix} \Omega_*^2 + 2\Omega_*^2 - U_{yy}^0 \\ \Omega_*^2 + 2\Omega_*^2 - U_{yy}^0 \end{Bmatrix} \tag{10}$$

Since $U_{xx}^0 \neq U_{yy}^0$, the trajectory will be an ellipse centered on the L_2 point. The required radiation pressure acceleration may be obtained as

$$a_0 = \cos^{-3}\gamma \left[\frac{\Omega_*^4 - \Omega_*^2(U_{xx}^0 + U_{yy}^0 + 4) + U_{xx}^0 U_{yy}^0}{U_{yy}^0 - 2\Omega_* - \Omega_*^2} \right] \xi_0 \tag{11}$$

The uncoupled out-of-plane motion defined by Eq. (8c) may now be solved by Laplace transforms to give a general solution of the form

$$\begin{aligned} \zeta(t) = \zeta_0 \cos(\omega t) + \left(\frac{d\zeta}{dt}\right)_0 (U_{zz}^0)^{-1/2} \sin(\omega t) \\ + a_0 \cos^2\gamma \sin\gamma (U_{zz}^0)^{-1}[U(t) - \cos(\omega t)] \end{aligned} \tag{12}$$

where $U(t)$ is the unit step function and $\omega = (U_{zz}^0)^{1/2}$. Choosing $(d\zeta/dt)_0 = 0$, the solution can be more conveniently expressed as

$$\begin{aligned} \zeta(t) = U(t) a_0 \cos^2\gamma \sin\gamma (U_{zz}^0)^{-1} + \cos(\omega t) \\ \times [\zeta_0 - a_0 \cos^2\gamma \sin\gamma (U_{zz}^0)^{-1}] \end{aligned} \tag{13}$$

It can be seen from this form of the solution that once the sail is pitched from $\gamma = 0$ at $t = 0$ the motion is of the form of periodic oscillations at an out-of-plane distance $a_0 \cos^2\gamma \sin\gamma (U_{zz}^0)^{-1}$. By choosing the initial out-of-plane distance $\zeta_0 = a_0 \cos^2\gamma \sin\gamma (U_{zz}^0)^{-1}$, the sail remains at this fixed distance. The ζ component of the radiation pressure acceleration, and so the out-of-plane distance, may be maximized by an optimal choice of sail pitch angle γ^*, viz.,

$$\frac{d}{d\gamma} a_0 \cos^2\gamma \sin\gamma = 0 \Rightarrow \gamma^* = \tan^{-1}(2^{-1/2}), \quad (\simeq 35°.264) \tag{14}$$

Using this optimal pitch angle, the sail may execute an out-of-plane elliptical trajectory centered at the L_2 point.

The sail may be placed on such a trajectory by inserting it into a suitable elliptic path about the L_2 point. Once the sail is pitched to an angle γ^*, the out-of-plane oscillations may be damped in a time optimal manner. The optimal damping of such a system has been considered by Bryson and Ho.[10]

Applications

A moderate performance solar sail on such an out-of-plane ellipse could be used to demonstrate the use of the L_2 point for lunar far-side communications. At an out-of-plane distance of 3.5×10^3 km, both the lunar far-side and the equatorial regions of the Earth would be visible, requiring a sail acceleration on the order of 0.2 mms^{-2}. The trajectory itself would be a narrow ellipse with semimajor and minor axes of 1.105×10^4 km ($\eta_0 = 2.876 \times 10^{-2}$) and 5.655×10^2 km ($\xi_0 = 1.471 \times 10^{-3}$) and a period of 29.53 days (synodic lunar month); see Fig. 2. Since trajectories in the neighborhood of the lunar L_2 point are naturally unstable, active control will be required to ensure damping of the divergent modes. Also, the neglected nonlinear terms in Eqs. (8) will perturb the sail from its nominal elliptic trajectory. Even allowing for the idealizations of the dynamical model though, it is proposed that such a trajectory could be flown with the solar sails now being designed for the solar sail Moon race.

Acknowledgment

This work was carried out with the support of a Royal Society of Edinburgh Robert Cormack Fellowship.

References

[1]Friedman, L., et al., "Solar Sailing—The Concept Made Realistic," AIAA Paper 78-82, Jan. 1978.

[2]Sauer, C. G., "Optimum Solar Sail Interplanetary Trajectories," AIAA Paper 76-792, Aug. 1976.

[3]Forward, R. L., "The Statite: A Non-Orbiting Spacecraft," AIAA Paper 89-2546, July 1989.

[4]McInnes, C. R., and Simmons, J. F. L., "Halo Orbits for Solar Sails—Dynamics and Applications," *ESA Journal,* Vol. 13, No. 3, 1989, pp. 229–234.

[5]McInnes, C. R., and Simmons, J. F. L., "Solar Sail Halo Orbits I: Heliocentric Case," *Journal of Spacecraft and Rockets*, Vol. 29, No. 4, 1992, pp. 466–471.

[6]McInnes, C. R., and Simmons, J. F. L., "Solar Sail Halo Orbits II: Geocentric Case," *Journal of Spacecraft and Rockets*, Vol. 29, No. 4, 1992, pp. 472–479.

[7]Perret, A., LaBombard, E., and Koryo, M., "The Solar Sail Race to the Moon," IAF Paper 89-539, Oct. 1989.

[8]Vonbun, F. O., "A Hummingbird for the L_2 Lunar Libration Point," NASA TN-D-4468, April 1968.

[9]Farquhar, R. W., "The Control and Use of Libration Point Satellites," NASA TR-R-346, Sept. 1970.

[10]Bryson, A. E., and Ho, Y.-C., *Applied Optimal Control,* Blaisdell, Waltham, MA, 1969, pp. 156–157.

Antoni K. Jakubowski
Associate Editor

Dynamic Response Spectra for an Aerospace Payload and its Attachments

Gina Lee-Glauser* and Goodarz Ahmadi†
Clarkson University, Potsdam, New York 13699

Nomenclature

$A(X)$ = cross-sectional area
a = nonuniformity constant
C_o = payload damping coefficient
G = shear modulus
K = geometry constant factor
L = total height of the payload
m_o = mass of the payload
m_s = mass of the secondary system
N = number of modes
q_n = modal amplitude
u = deflection of the payload relative to its base
$\ddot{u}_l$ = launch vehicle acceleration
X = distance from the base
x = dimensionless height
$z(t)$ = subsystem displacement relative to the payload
ζ_n = payload damping coefficient
ζ_s = secondary system damping coefficient
λ_n = payload eigenvalue
ρ_o = mass density per unit volume
ϕ_n = normal mode
ω_n = payload natural frequency
ω_s = secondary system natural frequency

Introduction

AN aerospace payload generally contains a number of highly sensitive and expensive subsystems such as satellite antennas, solar arrays, and other sensitive accessories. It

Received Aug. 16, 1991; revision received Oct. 25, 1991; accepted for publication Feb. 14, 1992.

*Graduate Student, Department of Mechanical and Aeronautical Engineering.

†Professor, Department of Mechanical and Aeronautical Engineering.